Detection of dense biomass burning area and the particle properties from GCOM-C / SGLI measurements

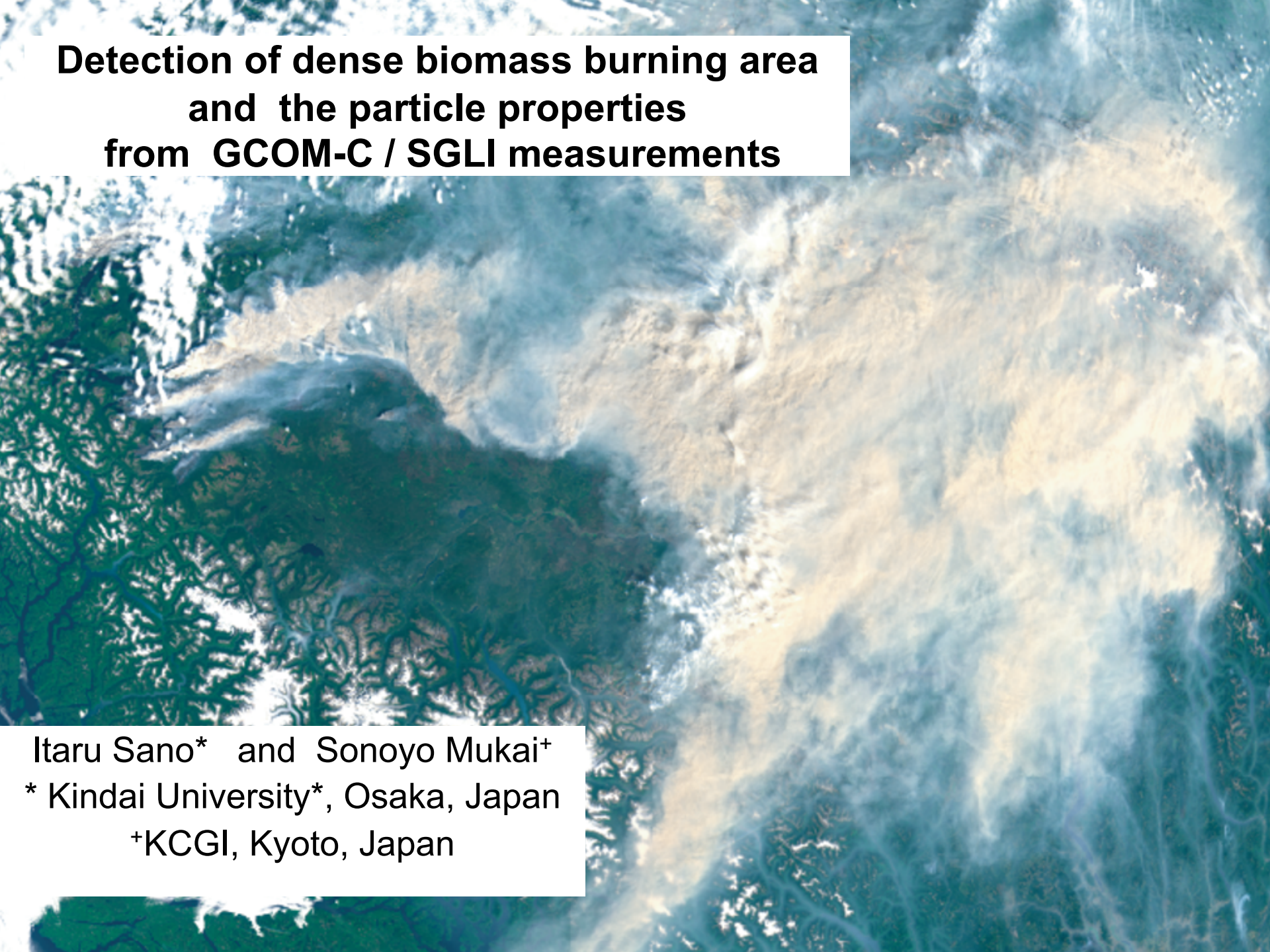

Itaru Sano* and Sonoyo Mukai+
* Kindai University*, Osaka, Japan
+KCGI, Kyoto, Japan

Background

Quantification of aerosol radiative forcing depends on the optical, chemical, and microphysical properties of carbonaceous aerosols.

Nowadays, severe aerosol events, e.g., wildfire smokes, dust storms, and volcanic plumes, influence on ecosystem as health and air quality.

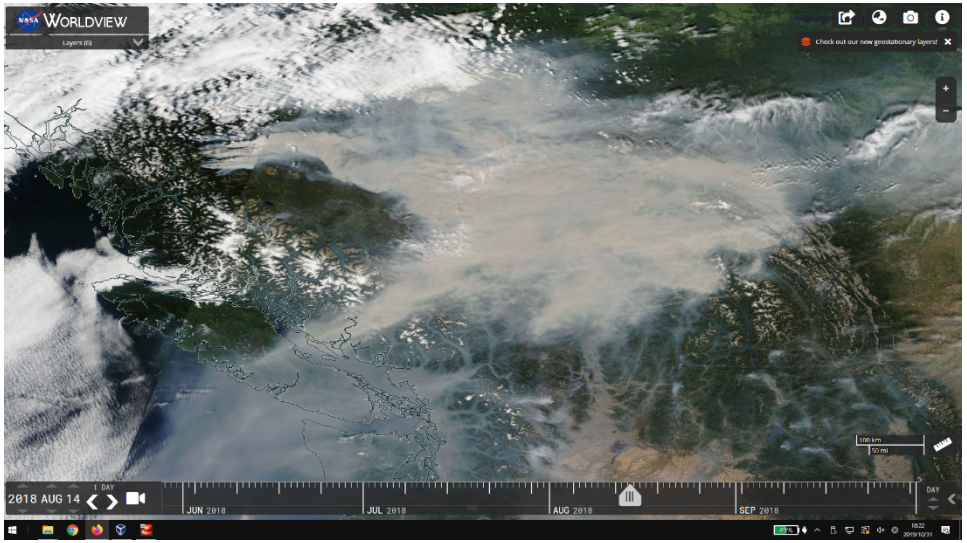

Worldview (MODIS) image on Aug. 14, 2018

Background

However, the details of such dense aerosols are not realized due to classify into haze or clouds.

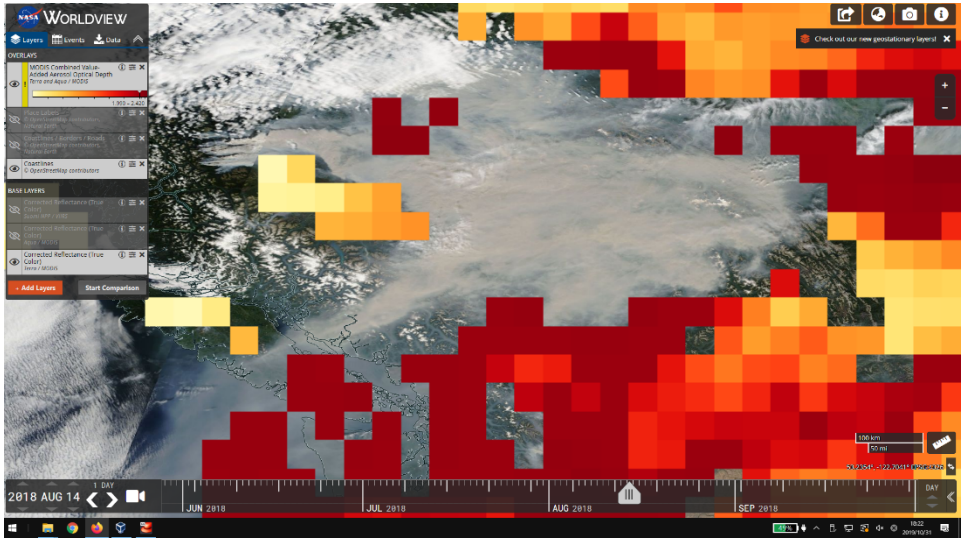

Worldview (MODIS-AOD) image on Aug. 14, 2018

Objectives (#1)

1. Detection and classification of absorbing aerosols

Biomass burning aerosols (BBA)

Mineral dusts (DUST)

Algorithm has been proposed based on

Japanese MODIS like sensor, GLI on ADEOS-2 (2002),

adapts to Second GLI (SGLI) on GCOM-C (2017).

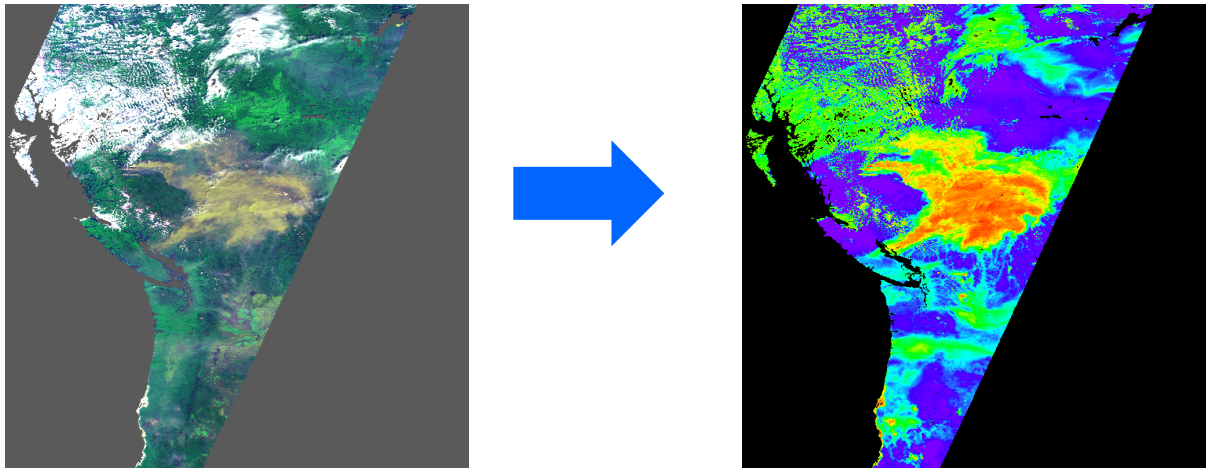

Objectives (#2)

2. Retrieving aerosol properties over dense aerosol region

Ångström exponent (AE)

Single scattering albedo (SSA)

based on semi-infinite atmosphere model by

Vector version of Method of SOS (VMSOS).

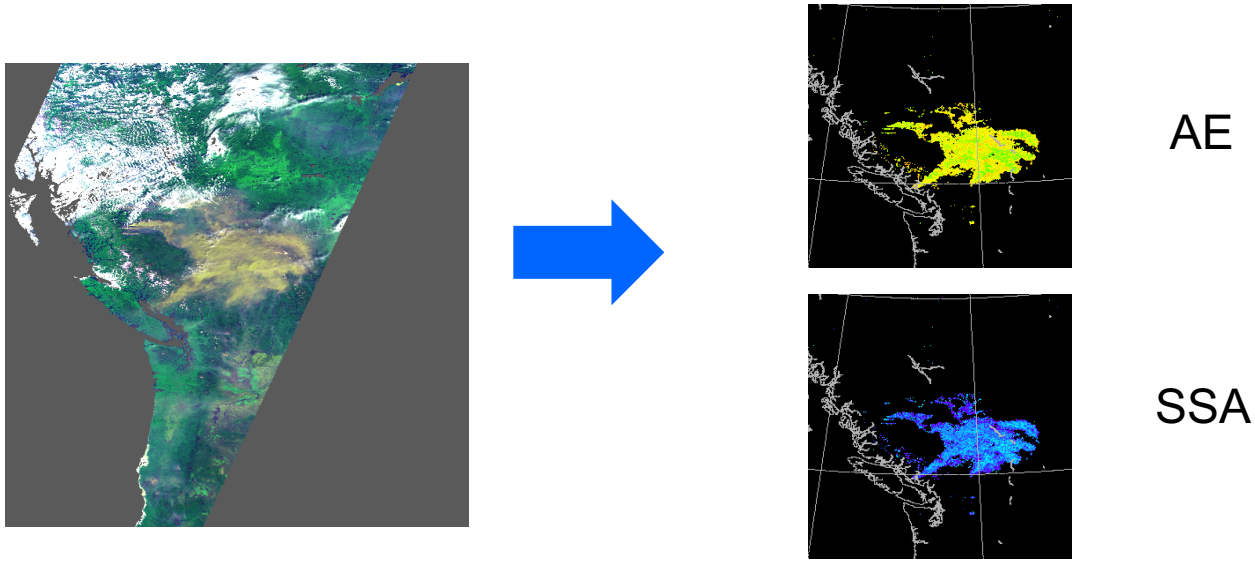

Classification of aerosol type

Absorbing aerosols in UV are discriminated from other type

AAI = R(412) / R(380) Absorbing aerosol index (AAI)

Separation of dusts (Dust) from biomass burning aerosols (BBA)

DDI = R(2210) / R(380) Dust detection index (DDI)

A discrimination chart
of aerosol types

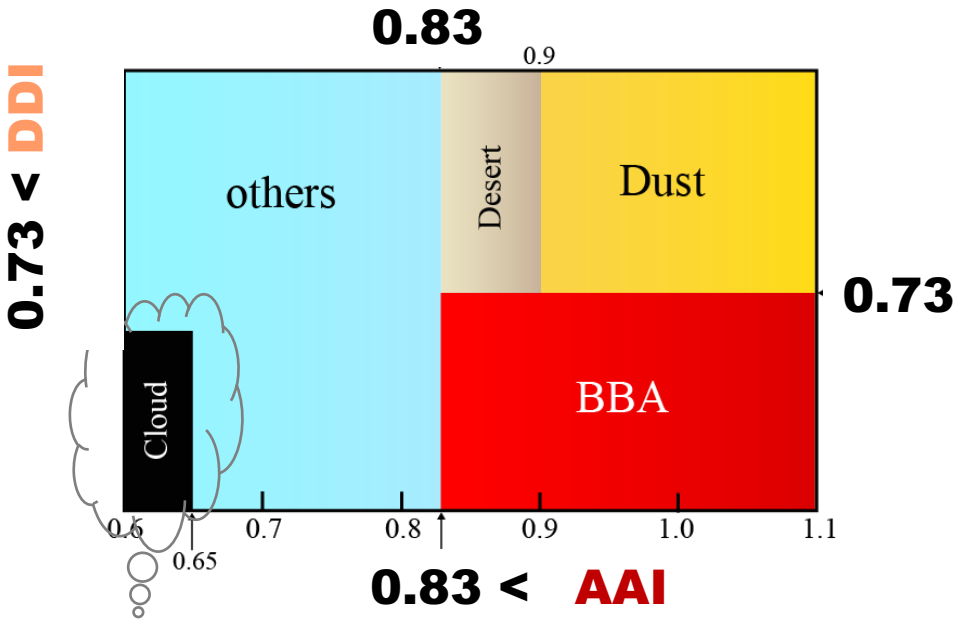

Optically thick cloud
as COT(0.67)≥20

* Mukai, S., Sano, I. and Nakata, M.: *J. Appl. Rem. Sen.* 13(1), 014527, doi:10.1117/1.JARS.13.014527, 2019.

Extension of aerosol type classification to SGLI / GCOM-C, 2017

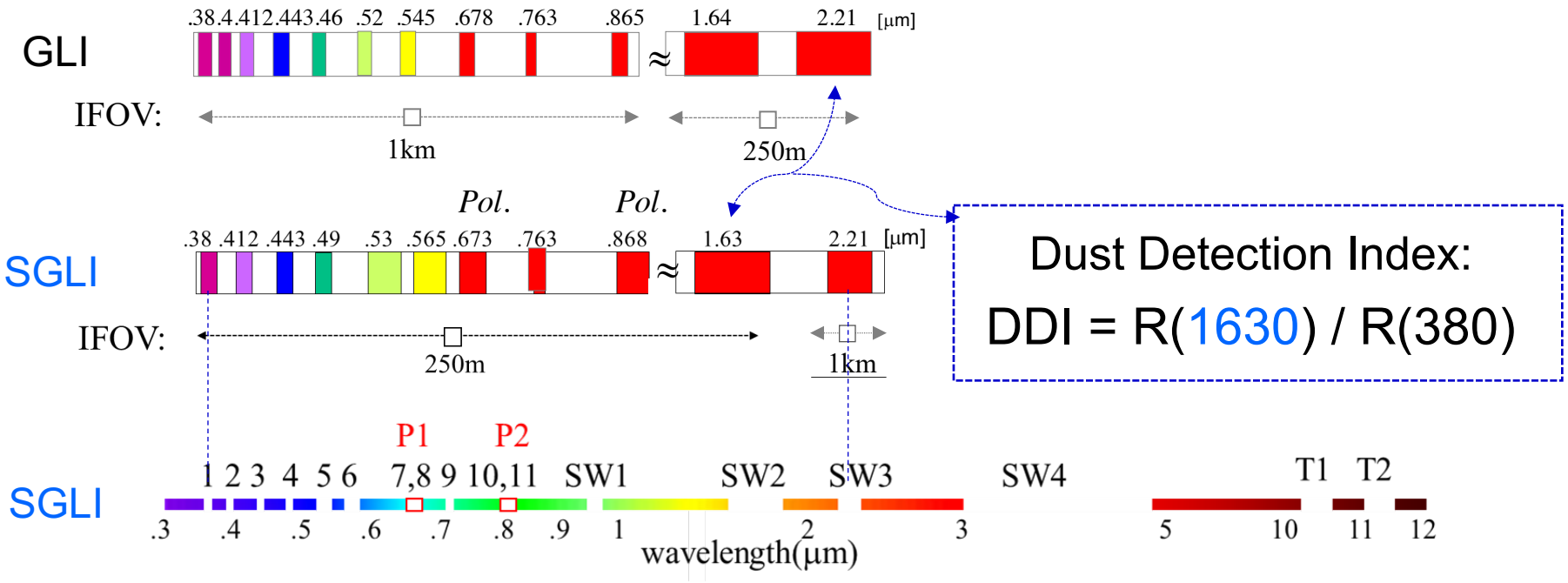

In a similar manner to ADEOS-2/GLI (2002) case, a discrimination chart of aerosol type classification is examined using GCOM-C/SGLI data (2017).

Detection of absorbing aerosols : discrimination of BBA and DUST

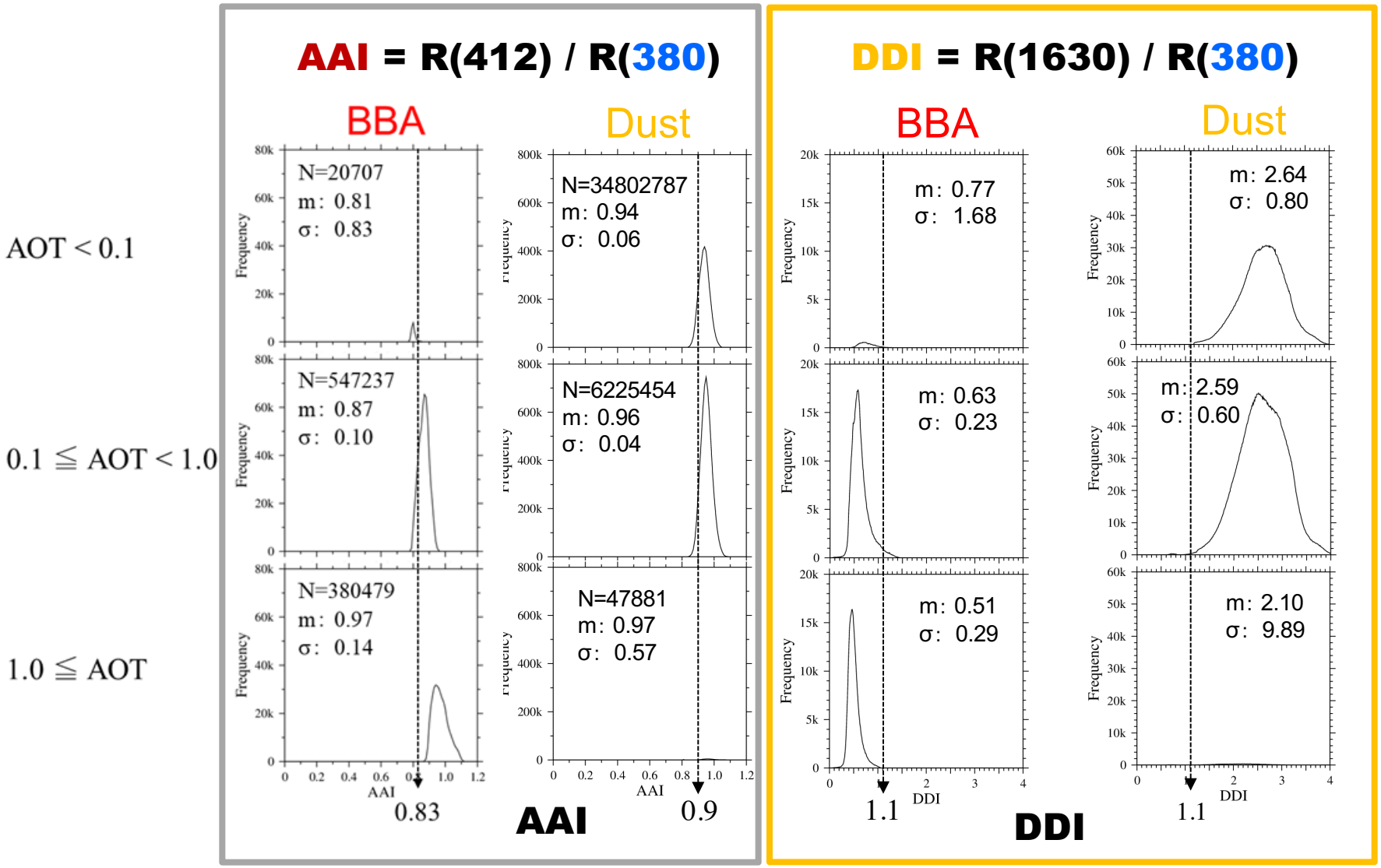

GCOM-C/SGLI (L2) data
from 1 May 2018 to 23 August 2019

Dependency of color ratio on AOT(500nm)

BBA

N= 948423

(Africa, Amazon, Siberia, etc.)

Dust

N=9753613

(Sahara Desert)

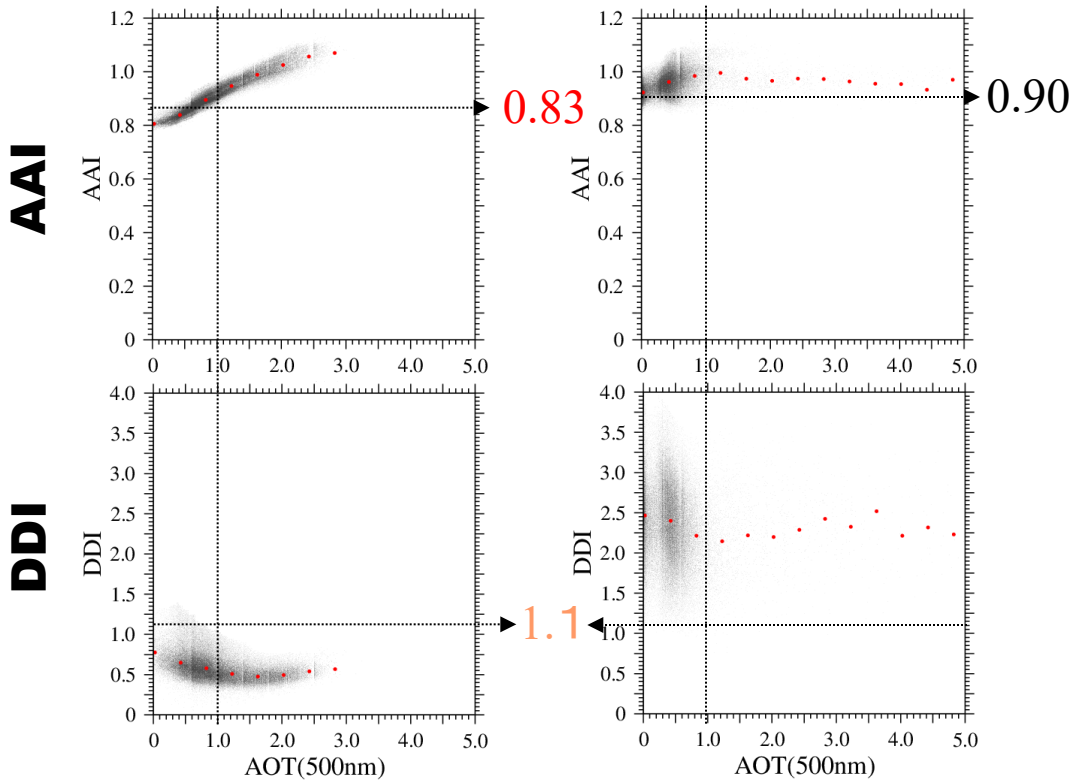

GCOM-C/SGLI (L2) data
from 1 May 2018 to 23 August 2019

Discrimination chart of aerosols type from SGLI

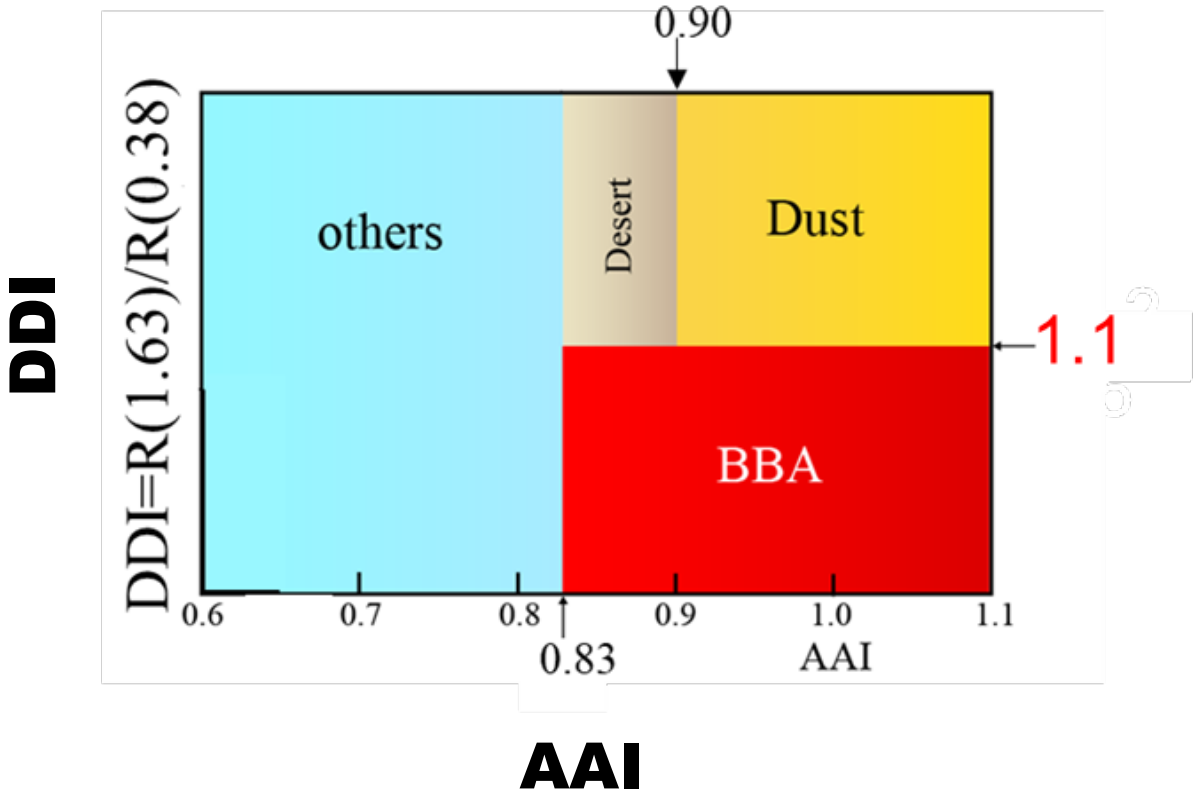

SGLI imagery on Aug. 14, 2018

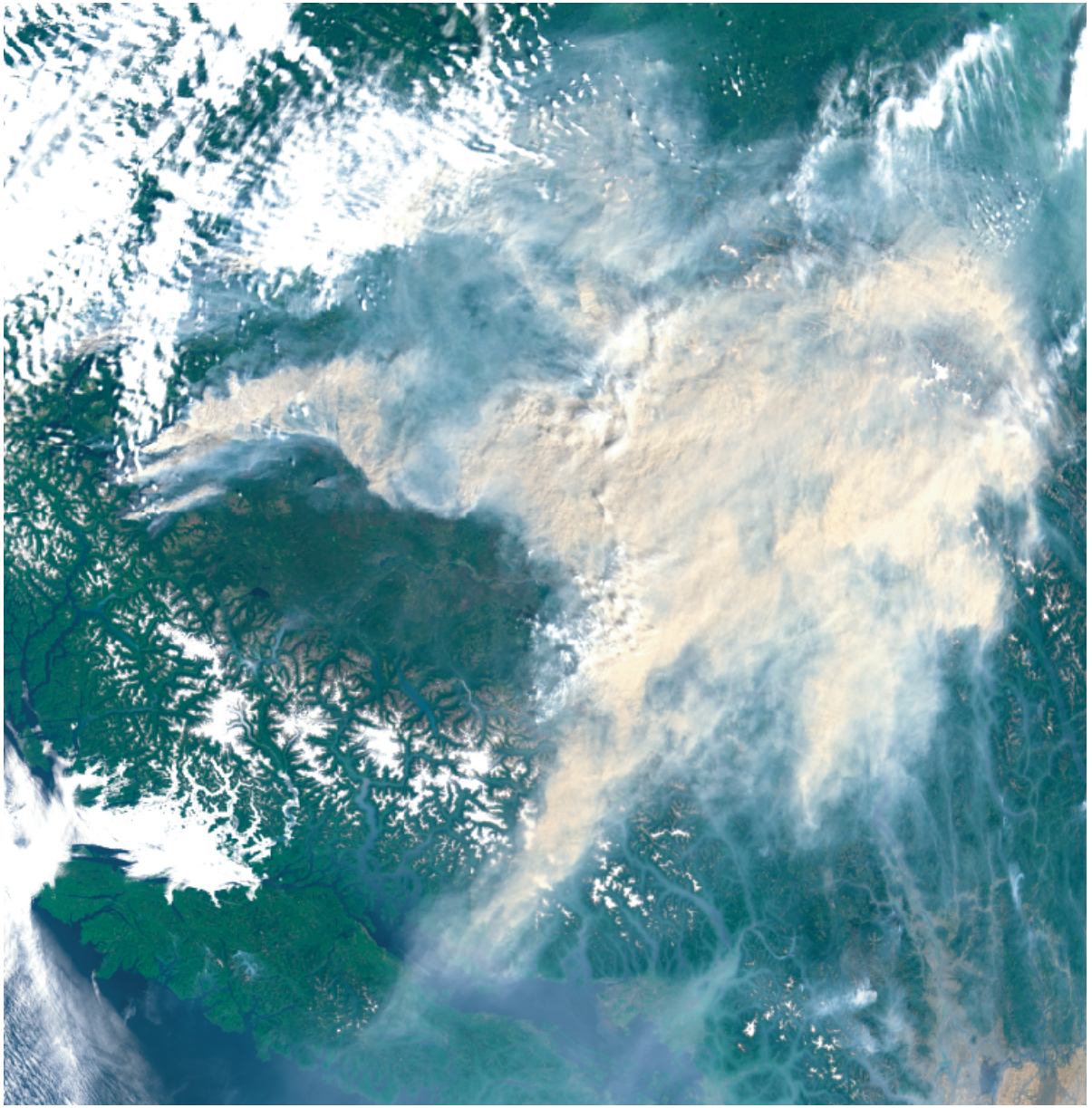

Characteristics of BBA type in Western Canada on Aug. 14, 2018

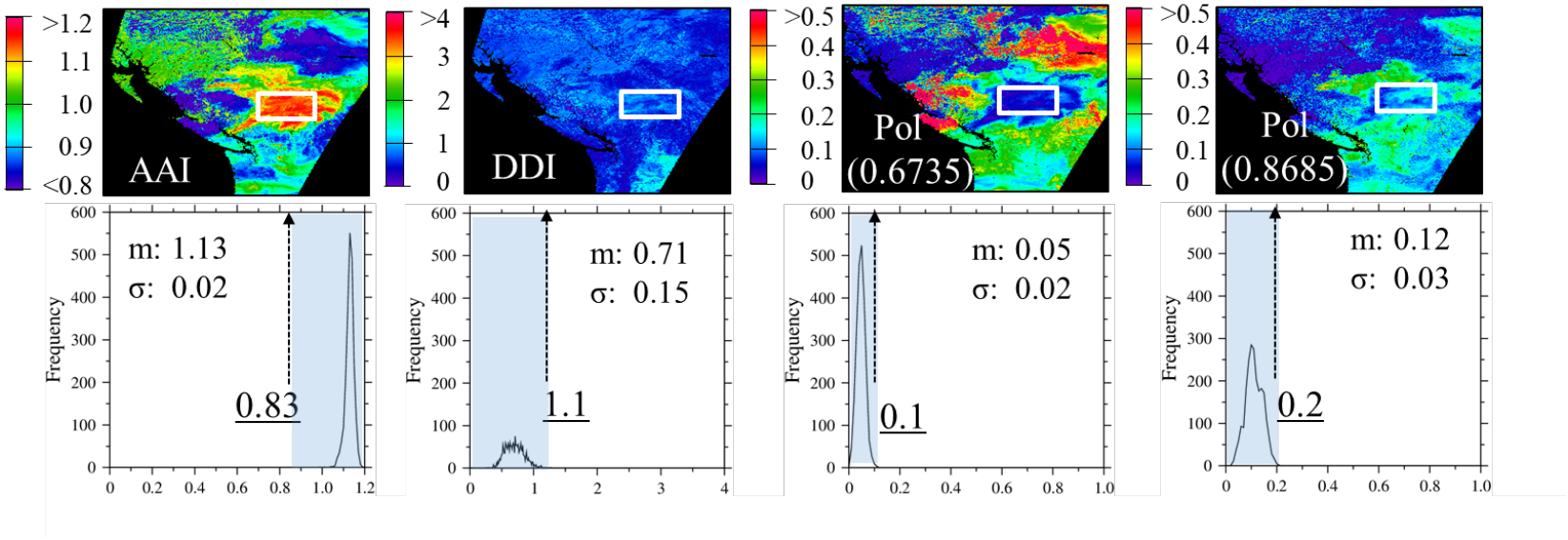

The BBA episode in western Canada coincides with the discrimination chart using AAI and DDI indices from SGLI global data.

#2 Aerosol retrieval part

Radiative Transfer in coupled atmosphere-surface system is roughly divided into 2-cases with respect to AOT(τ)

R. T. equation ;

$$\mu \frac{d\boldsymbol{I}(\tau,\Omega)}{d\tau} = \boldsymbol{I}(\tau,\Omega) - \frac{\omega}{4\pi}\int \tilde{P}(\Omega,\Omega')\,\boldsymbol{I}(\tau,\Omega')\,d\Omega'$$

should be solved

a) for infinite case: $\tau \sim \infty$

ex) aerosol events
dust storm /
biomass burning

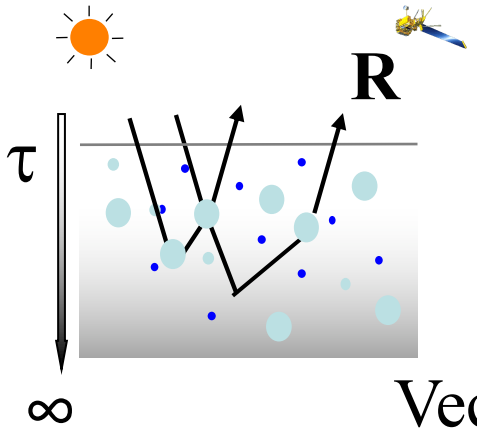

VMSOS:
Vector - Method of
Successive Order of Scattering

b) with boundary conditions for finite atmosphere

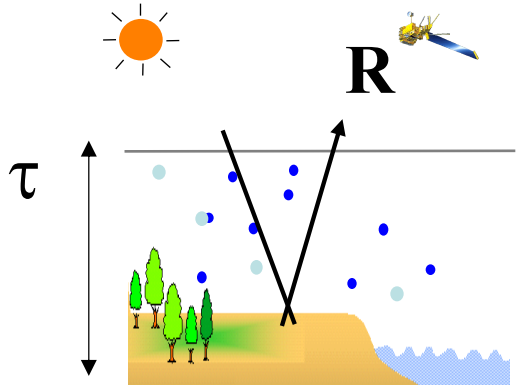

a) VMSOS; RT algorithm for semi-infinite atmosphere model in the polarization field

$$\tilde{R} = \sum_{i=1}^{\infty} \omega^n \, \tilde{R}^*(n)$$

ω : albedo for single scattering

$R^*(n)$: n^{th} - order of reflection *fn.*

number of scattering

n =1, 2 3 ... ∞

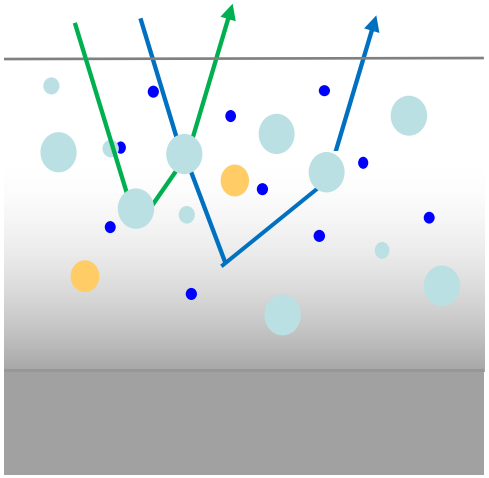

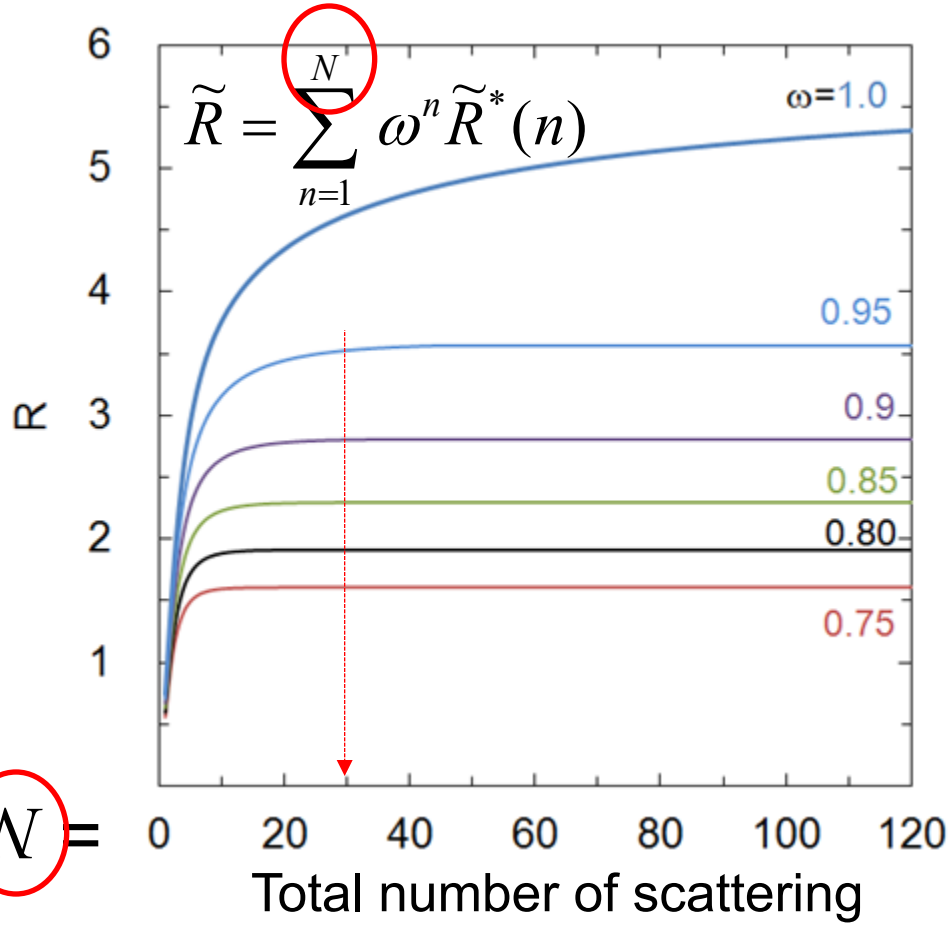

VMSOS convergence indication → N =

Aerosol modeling based on AERONET

Size distribution : Bi - modal log-normal function

(Omar et al. JGR, 2005)

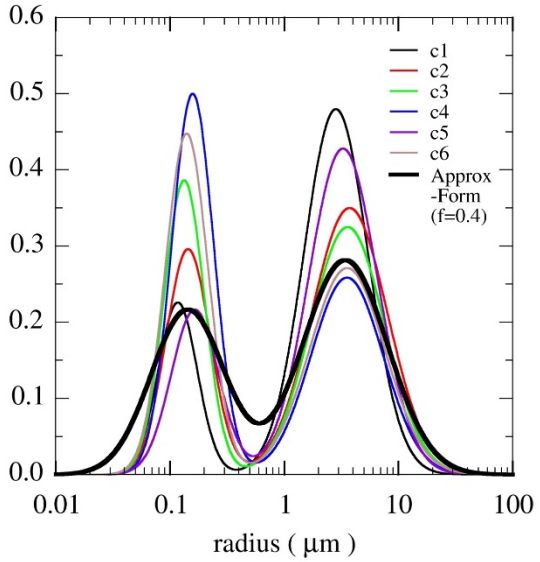

aerosol type	small		large	
	$\overline{r}_f$	σ_f	$\overline{r}_c$	σ_c
BB	0.144	1.562	3.733	2.144
RU	0.133	1.502	3.590	2.104
CP	0.158	1.526	3.547	2.065
DP	0.140	1.540	3.556	2.104
AF	**0.144**	**1.533**	**3.607**	**2.104**

Complex refractive index ($m = n - ki$) :

n : 1.50 (fixed)

k : 0.0001 - 0.1 (7 values)

Optical properties of Biomass burning aerosols

over Alaska (Bonanza), Amazon (JI_Parana_SE)

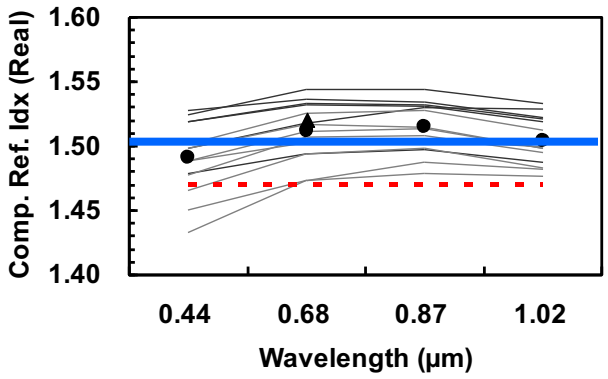

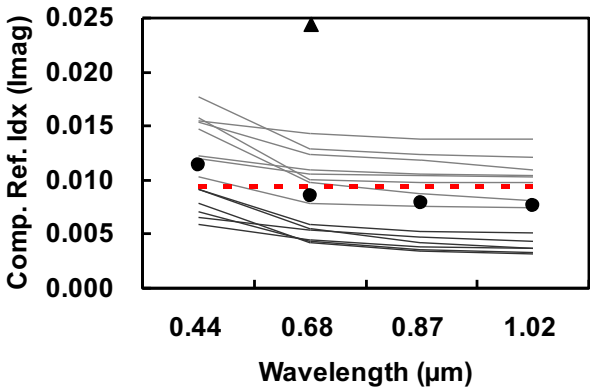

2004/6/27 1.193
2004/8/17 2.393
2004/8/20 2.436
2005/8/12 1.533
2005/8/16 2.255
2005/8/19 0.633
2006/8/24 0.648
2007/9/12 2.302
2010/8/14 1.136
2010/8/17 0.549
2010/8/20 1.080
2010/8/22 1.583
2010/9/7 1.135
2010/9/8 0.879
Average
Omar Category 2
Dubovik Biomass

$\tau_{500} > 0.4$

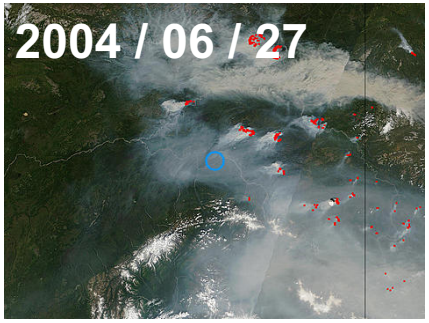

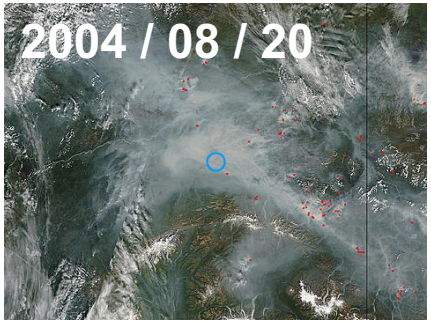

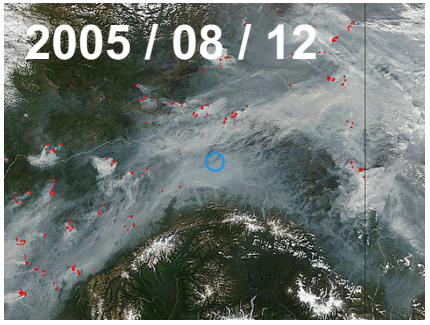

0.44um	1.491-0.0114i
0.67um	1.512-0.0085i
0.87um	1.515-0.0079i
1.02um	1.505-0.0077i

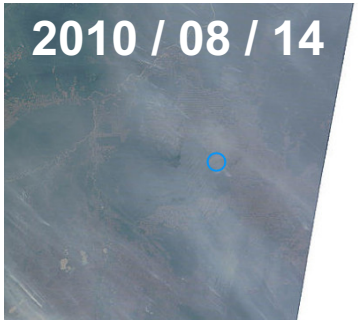

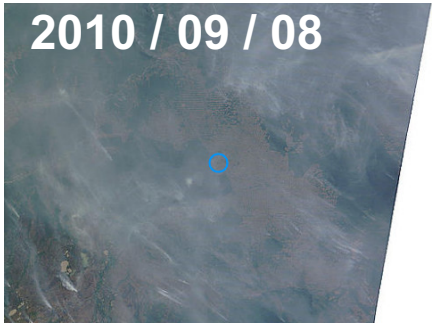

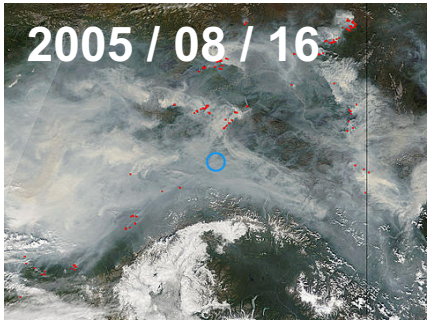

Aerosol modeling based on AERONET

Size distribution : Bi - modal log-normal function

(Omar et al. JGR, 2005)

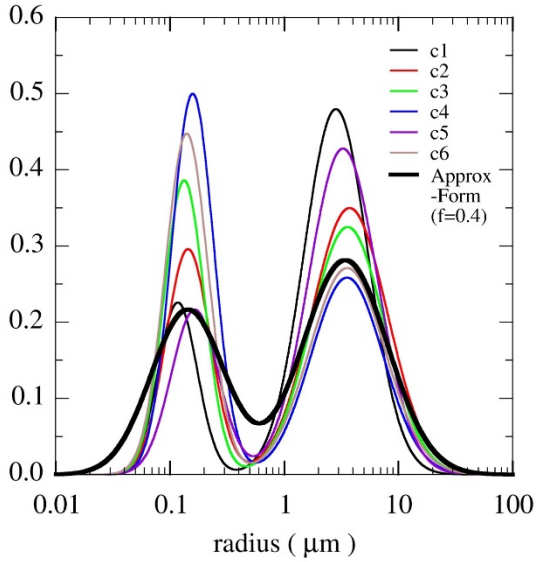

aerosol type	small		large	
	$\overline{r}_f$	σ_f	$\overline{r}_c$	σ_c
BB	0.144	1.562	3.733	2.144
RU	0.133	1.502	3.590	2.104
CP	0.158	1.526	3.547	2.065
DP	0.140	1.540	3.556	2.104
AF	**0.144**	**1.533**	**3.607**	**2.104**

Complex refractive index ($m = n - ki$)

n : 1.50 (fixed)

k : 0.0001 - 0.1 (7 values)

a) Aerosol retrieval by VMSOS : inputs and outputs

Inputs :

Nadir view SGLI measurements at 380, 412, and 530 nm.

Retrieved properties:

CMF of bimodal size dist.,

Imag. part of complex ref. idx.

Outputs:

→ Angstrom Exponent (AE),

and SSA (380, 530 nm)

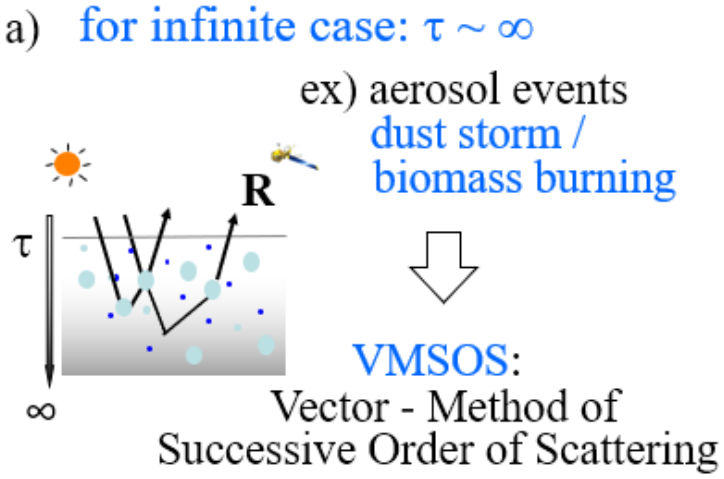

Retrieval of aerosol properties over western Canada on Aug. 14, 2018

Ang Exp (AE)

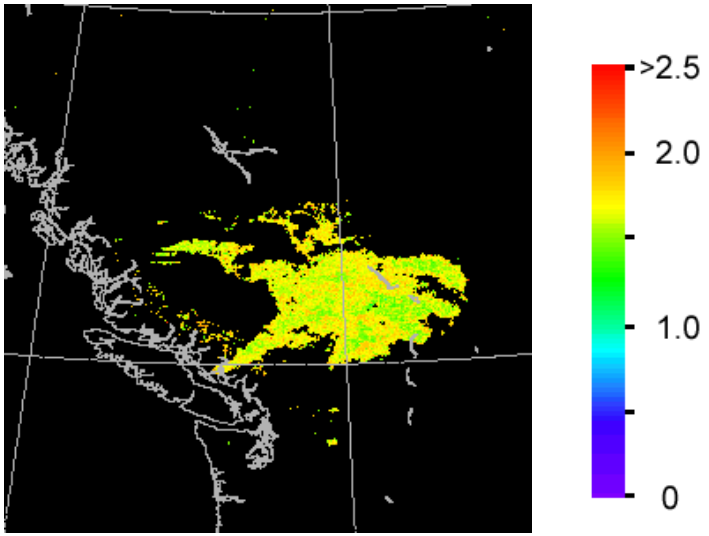

SSA (380 nm)

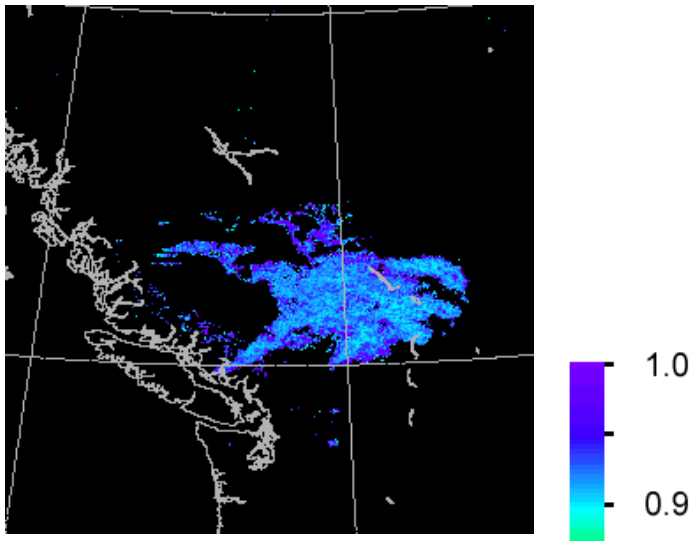

SSA (530 nm)

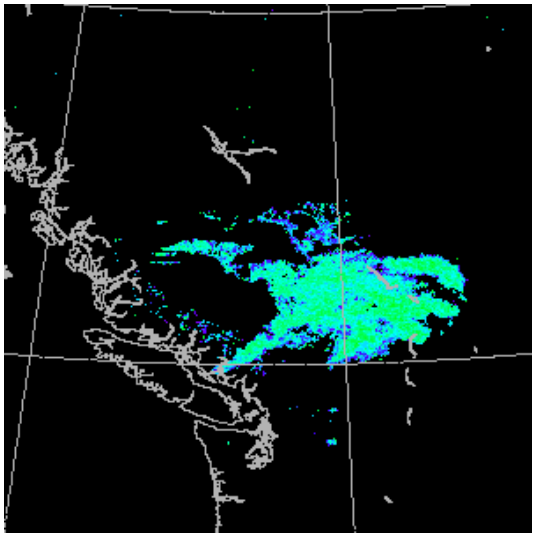

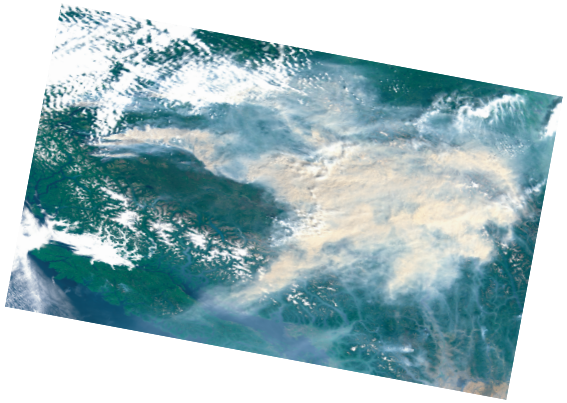

b) Aerosol retrieval for finite atmosphere model

Inputs :

Retrieved CMF, complex refractive index (m) from VMSOS

Nadir view SGLI measurements at 380, and 530 nm.

Retrieved properties:

AOT 550 nm

b) with boundary conditions for finite atmosphere

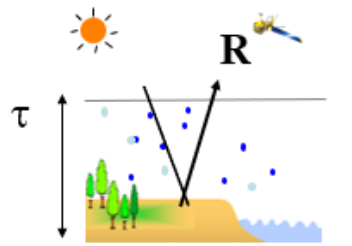

Outputs:

→ AOT (380, 412, 443, 530 nm)

Retrieval of aerosol properties
over western Canada on Aug. 14, 2018

AOT (380 nm)

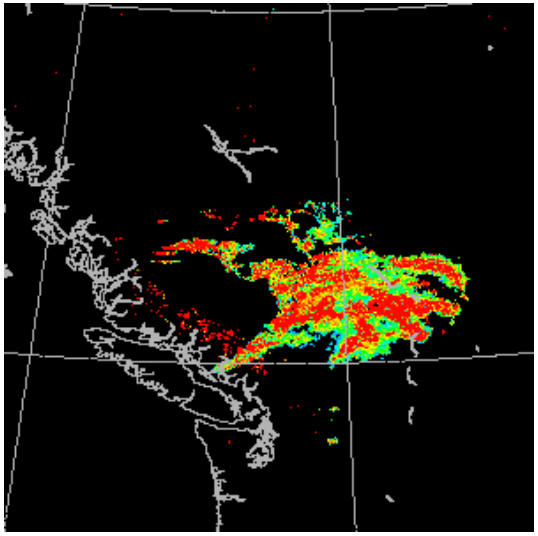

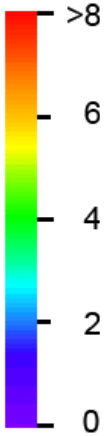

AOT (443 nm)

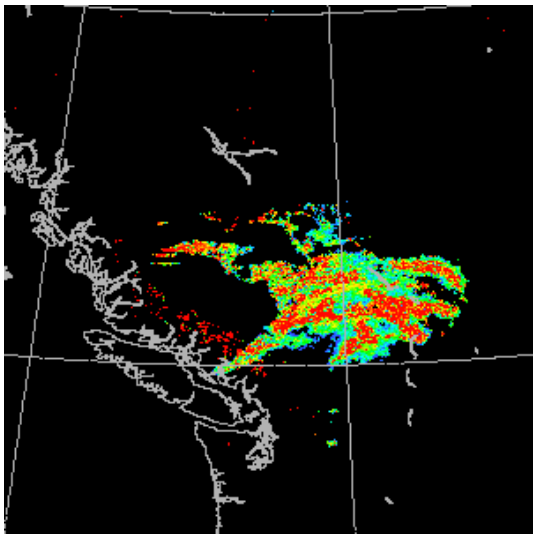

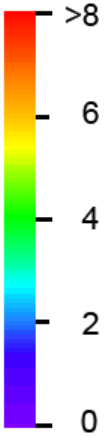

AOT (530 nm)

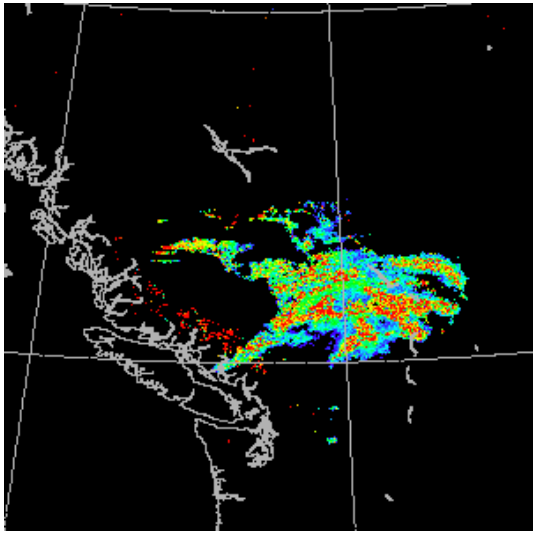

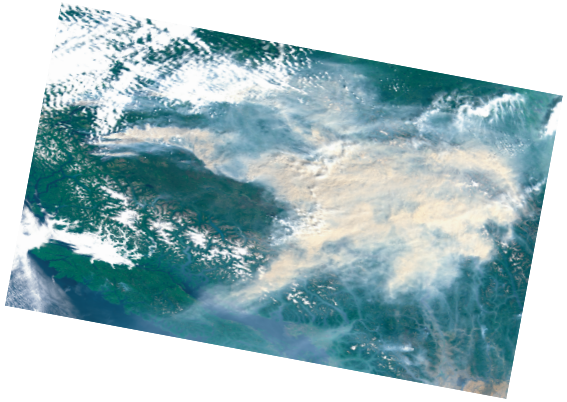

Summary

Detection and classification of absorbing aerosols based on color ratio of near UV (AAI, and DDI) is available for SGLI.

Radiation simulation algorithms are used for semi-infinite atmosphere model in the polarization field.

Aerosol properties as *Ångström exponent, SSA and AOT* are retrieved over dense aerosol region.

Further polarization information should be considered for efficient utilization.

Finally, I expect aerosol information from ground will be available by AERONET DRAGON campaigns.

Acknowledgements

The authors thank to JAXA for data distribution of GCOM-C/SGLI measurements.


BURGDORF